

JUN 8 1938

Library, L. M. a. L.



TECHNICAL MEMORANDUMS

NATIONAL ADVISORY COMMITTEE FOR AERONAUTICS

No. 864

4.5.1.1
4.7.3

LOAD TESTS ON A STIFFENED CIRCULAR CYLINDRICAL SHELL

By E. Schapitz and G. Krümling

Luftfahrtforschung
Vol. 14, No. 13, December 20, 1937
Verlag von R. Oldenbourg, München and Berlin

FILE COPY

To be returned to
the files of the Langley
Memorial Aeronautical
Laboratory.

Washington
May 1938



NATIONAL ADVISORY COMMITTEE FOR AERONAUTICS

TECHNICAL MEMORANDUM NO. 864

LOAD TESTS ON A STIFFENED CIRCULAR CYLINDRICAL SHELL

By E. Schapitz and G. Krümling*

For the purpose of checking and supplementing the theoretical computations carried out by the DVL (reference 1) on the force distribution in cylindrical shells, tests will be described in the present report whereby the stress distribution may be determined in a stiffened circular cylindrical shell loaded longitudinally at four symmetrically situated points. As being of particular importance are the cases investigated of groups of bending and arching or convexing forces, respectively. From the stress measurements on the longitudinal stiffeners, the shear stresses and the bulkhead ring stresses in the skin could be evaluated. These measurements showed that the "simple shear field" used in theoretical computations in which all normal stresses in the skin are neglected, must be extended by the addition of the transverse or circumferential stresses (denoted by σ_y) if the bulkhead rings are not riveted to the skin. The effect of buckling of the skin on the reduction of the stress disturbance within the load range investigated appeared to be slight. If the direct attachment to the skin of all of the bulkheads is loosened, the stress disturbance is reduced at a somewhat slower rate along the cylinder than is the case when the first two bulkheads are attached to the skin.

I. INTRODUCTION

The strength computations of shell or stressed-skin structures in airplane construction offer particular difficulties where concentrated forces must be applied at isolated points. The computation procedures that have so far been developed for cylindrical shells are based on

* "Belastungsversuche mit einer versteiften Kreiszyinderschale bei Krafteinleitung an einzelnen Punkten." Luftfahrtforschung, vol. 14, no. 12, December 20, 1937, pp. 593-606.

simplified concepts as to the shell structure, the stiffness of its parts, and the stress distribution. H. Wagner and H. Simon (reference 2), for example, consider the sheet metal walls between the stiffeners to be rigid with respect to shear and the peripheral stiffeners (bulkheads) as rigid with respect to normal forces, the rings being closely spaced and attached to the skin. H. Ebner and H. Köller (reference 1) consider the shell from the viewpoint of a system with multiple static indeterminacy. The normal stresses are thought of as concentrated in the stiffeners whereas the skin transmits only shear stresses ("simple shear field"). Within each of the fields or bays into which the skin is divided the shear stress is assumed as constant. Any longitudinal stresses through the skin can be taken into account by assuming an effective contributing width at the longitudinal stiffeners. The bulkheads are considered as connected to the skin and take up, in the form of tangential loads, the differences between the shears of two neighboring fields. With the simple shear field assumption, at least two bulkhead rings must be attached to the skin in order that a stable system be obtained. Bulkheads not attached to the skin cannot, if the setting up of peripheral skin stresses are excluded, take up any shear differences and will have no effect in reducing the stress disturbance. The latter depends essentially on the stiffness of the riveted bulkhead.

The object of the tests described in this paper was to check the validity of the assumptions made in the simplified scheme for the computation of cylindrical shells by carrying out measurements on a stiffened cylindrical shell. For this purpose, the actual stress distribution was to be determined and the stress measurements evaluated so that the shears and transverse stresses in the skin could be determined. The cylinder was loaded longitudinally at four points by forces which formed either two similarly directed couples constituting a group of bending forces or two oppositely directed couples constituting a group of convexing or arching forces (fig. 2). The first case is of importance in connection with bending stresses of fuselages, and the second, in connection with torsional stresses. In particular, the shear field was to be checked at those portions of the shell where the bulkheads were not riveted to the skin. For the case of arching type of loading there was also investigated the effect of loosening the connections of all the bulkheads to the skin. Further, for the two cases of loading there

was investigated the effect of buckling of the sheet covering and, for the case of the arching type of loading, the effect of adding a ring rigid in bending and torsion at the free end of the cylinder.

On the basis of the tests herein described, the "simple" shear field scheme of Ebnor and Köller is extended by the addition of the transverse circumferential stresses. There is also given a comparison between the computation and test results as regards the stresses in the longitudinal stiffeners while on figure 20 is given a comparison of the shears for the case of the arching type of loading.

II. TEST SET-UP AND PROCEDURE

The test specimen is a stiffened circular cylindrical shell of 800 mm diameter of a construction similar to that of the shells used in the DVL strength tests (reference 3). For taking up the applied concentrated forces, however, four symmetrically arranged longitudinal stiffeners of especially large cross section and to be denoted in what follows as "main spars" are symmetrically arranged about the cylinder (fig. 1). Between these, bay VI up to bulkhead f has been cut away above and below. At this "loading side" the concentrated forces are applied. In the horizontal plane the shell is longitudinally divided in order that other shapes of cut-outs, for example, those lying on one side only may be represented. For the purpose of having a simple schematic structure the main spars are of uniform cross section throughout the cylinder length, although in practical constructions a gradual weakening of the spars is customary. The two bulkheads e and f behind the cut-out have been designed stronger than the others and are riveted to the skin while the others are attached only to the longitudinal stiffeners. The positions where the main spars pass through the bulkheads are strengthened by riveted corrugated sheet. The skin thickness is 1 mm in bay VI, 0.8 mm in bay V and 0.6 mm in the remaining bays. The cylinder is tested by the bending and convexing forces, respectively applied as shown on the sketch (fig. 2). The bending load is applied by means of two pairs of forces symmetrically situated with respect to the center plane and having the lever arm $a = 49$ cm, the loading condition corresponding approximately to that of a monocoque fuselage acted upon by

the elevator forces. Figure 3 shows the test set-up. The loading machine is the same as in the previous tests except that there is an additional "loading cross" consisting of] [sections which distributes the moment to the four points of force application. The forces on the main spars are applied through inserted linings and angle pieces which transmit the compressive forces to the faces of the main spars (fig. 4). At the restraint side the cylinder is fixed by means of a restraining ring similar to those of the previous tests. The main spars, however, are specially attached through lining pieces.

For the arching type of loading, the two couples must be equal and oppositely directed. This type of loading occurs during torsion of fuselages. Since these couples are in equilibrium with each other, it is possible to hold the shell fixed at spars 3 and 7 on the loading side and apply the loading couple to spars 12 and 16. The shell is free from other external forces and is only supported at its free end to balance its weight (fig. 5). Figure 6 shows the details of the set-up. For the type of loading considered, several deviations of the test specimen were investigated. In one series of measurements a ring stiff in bending and torsion was placed at the end (fig. 5) and in another series of measurements the riveting of bulkheads e and f to the skin was loosened.

For all loading cases the stresses were measured at the sections indicated in figure 1, there being one measuring section in bays I to IV, two in bay VI and three in bay V. Figure 1 likewise shows the measuring stations at the stiffeners. The mean stiffener stresses for the main spars and all the intermediate stiffeners were determined by taking the mean value from the readings at stations n, o, and p, and for stiffeners 5 and 14 from the readings at stations q and r while the readings on the skin side s and t served as check readings and were not taken everywhere. The measuring apparatus used were Huggenberger and Okhuizen-Staeger extensometers having a magnification of about 1000 : 1 and a gage length of 20 mm which could be extended to 100 mm when very small stresses were to be measured. Since the stiffener walls were designed for strength (at least 1 mm thick) the falsification of the results previously observed as a result of geometrical changes in length did not arise.

III. THE CARRYING OUT OF THE TESTS AND THE TEST RESULTS

1. Loading by Group of Bending Forces

With the cylinder loaded in pure bending, buckling occurred at a bending moment of 173,800 kg cm in the most compressed bays, namely, those in the neighborhood of bulkhead b (fig. 1). Since the stress distribution in that region is approximately linear, the corresponding extreme fiber stress may be computed from the usual bending formula and is found to be 270 kg cm². This value for the cylinder considered in these tests would be obtained from the formula of Redshaw (reference 4) if, to take account of the prebuckling deformations, the theoretical buckling compressive stress for unstiffened circular cylindrical shells is reduced from $0.6 E s/r$ to about $0.2 E s/r$. The stress measurements were carried out in two ranges, one range extending to a bending moment of 164,500 kg cm, that is, up to just below the buckling limit, the second range up to a bending moment of 445,000 kg cm, limited by the available loading capacity of the loading machine.

The stresses in the longitudinal stiffeners were determined from the strain measurements. In order to obtain an idea of the effective width contribution of the skin, the stress moments obtained from the measurements were compared with the moment of the applied forces. It was then found that the mean normal stress in each bay may be set equal to the mean value of the longitudinal stresses in the two neighboring stiffeners before buckling in bays I to IV occurs. In bay V, which showed the greatest stress concentration in the main spars, the normal stress in the bays next to the main spars was to be set equal to the stress in the neighboring stiffeners. Aside from this, the sheet itself at the main spars did not contribute any support of the load for the full width between the rivets. In the buckling range satisfactory agreement was obtained between the stress moment and the applied force moment when the effective width of sheet for the buckled panel on the pressure side was substituted according to the Ebner formula (reference 3). Figure 7 shows the normal stress distribution over the height of the section. The strong stress concentrations at the loading side (bay V) gradually decrease toward the fixed end so that there is practically a linear stress distribution with height of section.

Figure 8 shows the variation of the longitudinal forces in the stiffeners over the cylinder length. In the longitudinal stiffeners between the main spars and the neutral axis (9 and 10, 4 and 15, respectively) the forces, after an initial rise, attain a maximum and then decrease again to the value which corresponds to the linear stress distribution over the section height. As is shown by figure 7, at the highest attainable load the decrease in the supporting ability of the buckled skin on the pressure side is still not great enough to affect the shifting of the neutral axis toward the tension side as had been previously observed (reference 3). Figure 9 shows the forces (divided by the applied force) in the main spars in the prebuckling and buckling stages plotted against the cylinder length. It may be seen that within the range investigated the form of the curves in the transition through the buckling condition does not change. No buckling of the walls which were mainly stressed in shear took place, but rather the buckling was restricted to those bays that were essentially under a compressive stress.

Figure 10 shows the buckling stresses in the bulkhead rings for the prebuckling condition. It may be seen that the mean normal stresses in bulkhead f are oppositely directed to those in bulkheads d and e. The bulkhead ring stresses decrease to zero toward the fixed end. That the ring forces must change their signs over the cylinder length may be seen from a consideration of the equilibrium of the shell cap over the main spars (fig. 11a). It is immediately evident that the bending stresses in the cut along the main spars form a couple with the shear forces so that for equilibrium the bulkhead ring forces must produce an opposite couple. This is possible, however, only when the stresses in the individual rings have opposite signs.

2. Loading Through a Group of Arching Forces

In applying a group of "arching" forces the test specimen buckled in bay III between stiffeners 14 and 15 for an applied moment of 129,000 kg cm. In the prebuckling condition, the upper load limit was found to be 115,700 kg cm. After the buckling limit was exceeded ring f failed by buckling close to main spars 7 and 16 at a convexing moment of 276,000 kg cm. For the measurements in the buckling range, the ring was reinforced and the upper limit of the measuring range was found to be at

a torsional moment of 232,000 kg cm. When the test cylinder was loaded without ring at the free end a strong elliptical bulging was observed (fig. 12).

There will first be considered the case where there is no stiff ring at the end so that the cross section is not hindered from bulging. Figure 13 shows the variation of the forces (divided by the area of the load section) in the longitudinal stiffeners over the cylinder length. In the main spars the forces decrease at first rapidly, then more slowly to the value zero and at rings e and f these curves exhibit abrupt changes. The forces and stresses in the remaining longitudinal stiffeners remain small, vanishing at the two ends of the cylinder and with a maximum value occurring in between. Figure 14 shows the typical longitudinal stress distribution over the cross section height for each of the measuring sections. The ring stresses are shown on the right half of figure 15. There may be seen a great increase in the bulkhead ring stresses toward the free end with reversal of stress sign between rings e and f. If the cylinder is assumed to be cut lengthwise at two oppositely lying main spars (fig. 11b) it is immediately evident that the section forces in the rings must produce a resultant couple. The great increase in the bulkhead stresses toward the free end will be explained in section IV.

The effect of a ring rigid in bending and torsion placed at the free end is to produce excess longitudinal forces in the spars at the free end (fig. 17). The stress of rings a to d is almost entirely relieved (fig. 15, left half) and that of ring f considerably decreased. Figure 16 shows that the rate of decrease of the forces within the range investigated (up to 1.8 buckling load) does not change essentially for the buckling range. As in figure 9, the forces are divided by the applied force in each main spar. In order to test the validity of the simple shear field scheme the stresses were also measured for the case where the riveting between the two foremost rings and the sheet covering was loosened. In this condition no shear can be transmitted at any position from the sheet to the stiffener and, if the simple shear field scheme were strictly correct, the shell must be an unstable system. In the case of a stiff end ring, the spar must be constant up to the end ring. Figure 17 shows the test results for the main spar. The abrupt breaks in the force curves at the first rings (f and e) disap-

pear and the spar forces decrease at a somewhat lower rate than for the riveted rings. With the end ring mounted, the forces in the main spars at the end ring are unchanged as compared with the case of riveted rings. The buckling strength of the cylinder likewise changes only slightly. The stability of the shell therefore does not depend on the riveting of the rings to the skin. Extension of the simple shear field through the addition of the circumferential stresses and the assumption of variable shear in the panels is thus justified.

IV. THE DETERMINATION OF THE STRESS DISTRIBUTION

1. The Extended Shear Field

In the assumption of simple shear field $\sigma_x = \sigma_y = 0$ and $\frac{\partial \sigma_x}{\partial x} = \frac{\partial \sigma_y}{\partial y} = 0$ everywhere over the skin. The con-

stancy of the shear in the sheet bays follows from the fundamental equations for the two-dimensional state of stress (see under IV, 2). Shear differences can be taken up only at the stiffeners which are attached to the skin. In order to vary the shear over the cylinder length, the rings must be attached to the skin. Rings that are not attached to the skin cannot affect the stress distribution.

If this scheme is extended by the addition of the circumferential stresses it is possible for the shear to vary continuously over the cylinder length. A radial bracing of the skin, which is not rigid in bending, by means of longitudinal stiffeners and rings must here be assumed. The longitudinal stiffeners take up the radial components of the circumferential stresses as a distributed load and transmit them to the bulkheads. Stiffness in bending of both of the systems of stiffeners is therefore a necessary assumption for the setting up of transverse stresses and for the variation of the shear along the shell. In this radial bracing of the shell the question of the attachment of the rings to the skin does not enter.

In the statically indeterminate computation, displacement coefficients for the bulkheads have to be determined, the values of which affect the stress distributions, particularly in the case of arching type of loading. With

continuously varying shear over the length, the bulkhead ring loading depends only on the difference of the mean shear values of two neighboring bays. The displacement coefficients for the simple and extended shear field would be equal if in both cases the same mean values of the shear were taken and if the axis of the ring were at the center surface of the skin. The effect of ring eccentricity, which is always present, can be taken into account and the simple scheme can be extended also to the case where the rings do not lie close to the sheet (reference 1).

2. Fundamental Considerations on the State of Stress

The sheet may be assumed as being essentially under a two-dimensional stress distribution. The state of stress is therefore determined by giving the normal stresses σ_x and σ_y (longitudinal and peripheral stress, respectively) and the shear stress τ . These stress components must be determined at each point of the cylinder covering for a complete picture of the stress distribution to be obtained.

The longitudinal stresses σ_x were measured at the longitudinal stiffeners and may be estimated in the bays of the sheet covering. The components σ_y and τ must be computed. To compute these there are available, for the sheet bays of constant thickness, the fundamental equations for the two-dimensional stress field.

$$\frac{\partial \sigma_x}{\partial x} + \frac{\partial \tau}{\partial y} = 0 \quad \text{and} \quad \frac{\partial \sigma_y}{\partial y} + \frac{\partial \tau}{\partial x} = 0 \quad (1)$$

In the longitudinal stiffeners, the longitudinal force P_x is altered by the shears of the riveted sheet bays (thickness s). Denoting by τ_b and τ_a the shear stresses at the two sides of the stiffener section there is obtained from the equilibrium of an element

$$\tau_b - \tau_a = -\frac{1}{s} \frac{d P_x}{d x} \quad (2)$$

For constant shear stresses, the force P_x thus varies

linearly with x . For every discontinuity in the shear distribution over x the corresponding curve $P_x(x)$ receives a break.

The shears will be discontinuous over x whenever the bulkheads riveted to the skin receive a tangential load (in the peripheral direction). The corresponding breaks in the P_x curves were observed during the loading by the arching forces (figs. 13, 16, and 17), whereas with the bending loads they did not occur (figs. 8 and 9). At all the free rims at which the shear could not be transmitted to a riveted longitudinal or transverse stiffener τ becomes equal to zero. As a result, there is also a vanishing of the slopes of the $P_x(x)$ curves at all free rims.

The moment check in the bending case gave the result that, in the prebuckling stage for a stress distribution continuous to a certain degree, the mean skin stress in a bay between two stiffeners could be set equal to the mean value of the stresses in these stiffeners. In the case of the convexing loading, the longitudinal stresses were measured near the main spars, the same values for these stresses being obtained as those for the longitudinal stiffeners near the main spars (for example, 11 and 13 or 15 and 17). At positions of great discontinuity of the longitudinal stresses in the peripheral direction, the bay stresses were therefore set equal to the smaller stiffener stress.

3. Determination of the Shear Stress

and the Transverse Stress from the Test Results

To determine the values of the forces P_x in the longitudinal stiffeners, there were available the measured values of the stresses σ_x . The supporting section may be assumed as made up of stiffener cross section together with the strip* of skin between the series of rivets. In bay V (see under III, 1) it appeared necessary to reduce this effective width of sheet at the main spars because at rings e and f the skin did not fully contribute in support. The factor determining the effective width was the equilibrium of the external and internal moments in the bending case.

*In what follows the term "strips" will be used to denote the sections of the sheet between longitudinal stiffeners while the term "bay" will denote the sections of the sheet between the bulkhead rings.

The curves $P_x(x)$ were graphically differentiated. The computation according to formula (2) gives the difference in the shear stress at the two sides of the longitudinal stiffener. Integration of the equation (1)

$$\frac{\partial \sigma_x}{\partial x} + \frac{\partial \tau}{\partial y} = 0 \text{ would give the shear stress distribution}$$

over the width b of the sheet bays if the normal stress distribution were measured or properly assumed. If the distribution of σ_x over the nondimensional peripheral coordinate y/b depends only on the values of σ_{x_1} and σ_{x_2} in the two peripheral stiffeners if, for example,

$$\sigma_x = \sigma_{x_1} - f\left(\frac{y}{b}\right)(\sigma_{x_1} - \sigma_{x_2}), \text{ then the derivative } \frac{\partial \sigma_x}{\partial x}$$

also depends only on the derivatives $\frac{d \sigma_{x_1}}{d x}$ and $\frac{d \sigma_{x_2}}{d x}$.

As was already mentioned, for continuous stress distribution we may set $f(y/b) = y/b$ (linear distribution) and at positions of sharp discontinuity assume σ_x as constant over the bay width [$f(y/b) = 0$ or $f(y/b) = 1$]. The shear increase over the width of a sheet bay is obtained as

$$\tau_2 - \tau_1 = - \int_0^b \frac{\partial \sigma_x}{\partial x} d y$$

If σ_x is to be assumed constant between the transverse stiffeners, then $\frac{\partial \sigma_x}{\partial x}$ is also constant over y .

Thus, at a section of the cylinder for each bay and for each stiffener, there may be computed a shear difference $\tau_2 - \tau_1$ or $\tau_b - \tau_a$. For the determination of the shear stresses themselves, an initial value is required. In the case of bending, this is obtained from the condition that, in the intersection of the shell with the vertical plane, the shear vanishes. In the case of the arching load, zero shear positions are obtained only at the main spars and the initial condition must be obtained from

the fact that $\int_0^{2\pi R} \tau dy = 0$ (twisting moment vanishes). In this case, the stress differences $\tau_2 - \tau_1$ are summed up

starting from an arbitrary zero value and the final zero line is so determined that the sum of the areas of the $\tau(y)$ curves over the semiperimeter (for example, between the intersections with the vertical plane) vanishes (the semiperimeter is sufficient on account of the antisymmetry of the stress distribution).

The shear stresses thus determined are plotted against the longitudinal coordinate x and the derivatives $\frac{\partial \tau}{\partial x}$ obtained graphically. For determining the transverse stresses, the equation

$$\frac{\partial \sigma_y}{\partial y} = - \frac{\partial \tau}{\partial x} \quad (1b)$$

is integrated with respect to y , it being necessary to determine initial values for the transverse stresses.

In the bending case the halves of the cylinder on each side of the horizontal plane are antisymmetrically loaded. The setting up of a peripheral stress in this intersecting plane would be contrary to the mutual interaction principle and therefore in the horizontal plane $\sigma_y = 0$. In the arching case both the vertical and horizontal planes are antisymmetric planes and hence free from transverse stresses. Maxima (over y) occur in the bending case in the section of the vertical plane

$\left(\frac{\partial \tau}{\partial x} = 0 \text{ for all values of } x \right)$ and in the arching case at the main spars.

The determination of the shear stresses may be checked by cutting the cylinder along the length and comparing the shearing forces in the intersecting planes with the applied forces (P at each spar, fig. 11) and the normal forces in the radial cuts. If in the bending case the cylinder is cut in the horizontal plane, then

$$\int_0^x \tau s \, dx = 2P - \int \sigma_x \, dF$$

where the integral of the shear-times-thickness is to be taken in the 2 cuts and the integral of the normal stresses extended over the half cross section. In the case of the arching loading the integral of the shear-times-thickness must be taken over the entire cylinder length and at all sections between spars 7 and 3 or between 12 and 16 must give the same force P_1 . Similarly the integrals in all sections between 7 and 12 or 3 and 16 must give the same force P_2 . The force at a spar is $P = P_1 + P_2$. This check is applicable if there are no stiff rings at the end.

4. Discussion of Results Obtained

a) Shear distribution.- According to the method here described, the shear stresses were computed for the case of the bending loading condition and for the arching loading condition at the upper limit of the below-buckling range. The stress distribution for the arching type of loading was investigated both for the case where the bulkheads e and f were attached to the skin as well as for the case where this attachment was loosened. Figure 18 shows the shear-times-thickness (based on an applied force at each main spar of $P = 1,000$ kg) plotted against the coordinate x in the longitudinal direction and against the coordinate y of the developed semiperimeter of the cylinder.

From the symmetry in the bending case of the stress field with respect to the vertical center plane the shear vanishes in the intersection with this plane. As a result of the antisymmetry with respect to the horizontal center plane, the shear distribution is symmetrical with respect to this plane. In the arching loading condition the vertical and horizontal planes are planes of symmetry for the shear distribution. In both of the loading conditions the shears change their signs in the main spars in going around the circumference. As may be seen on figure 18, the greatest shear is obtained for the arching load with bulkheads e and f unattached to the skin.

In all loading conditions, negative shears occur in bay VI in the strips at either side of the horizontal plane. In passing from the free edge to the full skin portion, the tension and compression stresses in the strips and in the intermediate stiffeners increase whereas the spar forces decrease. The resultant of the forces is thereby displaced at one side toward the neutral axis.

(See fig. 19.) The resultant force increases in magnitude because the moment applied remains constant. Such an increase, however, is only possible if there exists at the intersection with the horizontal plane a shearing action which is oppositely directed to that along the main spar.

In the bending load case the shear along the cylinder varies continuously; the distribution in the two inner strips (A and B) in bay V is related to the variation of longitudinal stresses in the stiffeners between the main spars and the longitudinal neutral axis. With the arching loading condition and with bulkheads e and f riveted, sharp discontinuities of shear occur in the latter ring. In the strips along the extreme fibers, the shear at first increases somewhat from bulkhead e toward bulkhead a and then again diminishes slowly to zero. In contrast to the bending loading condition, the changes in the shear between two main spars are not considerable and the change due to the longitudinal stresses in the strips negligibly small. If bulkheads e and f are unattached, the shears rise steeply in bay V to a maximum value and then again decrease steadily toward bulkhead a.

Under the arching loading condition with attached bulkheads, buckling occurs first in bay III, strip A' (figs. 1 and 18) for a spar load $P = 2630$ kg. The corresponding shear stress is obtained as $\tau = 128$ kg/cm². From the formula of H. Ebner (reference 3) the buckling strength of the sheet metal strip is obtained as 87.4 kg/cm² if the shear buckling strength is computed according to Donnell and 172 kg/cm² if it is determined by the formula of H. Wagner. The value computed from the test therefore lies in between. The fact that buckling first occurs in bay III and not in the somewhat more highly stressed bay IV may be explained by the effect of pre-buckling.

The check tests mentioned under IV, 3 were found to be in satisfactory agreement with the computed values of the shears, the deviations remaining within 10 percent of the applied spar forces.

The shears in the full skin portion in the peripheral direction generally vary little within a strip. An exception is formed by the strips which, in the bending case, lie in the neighborhood of the extreme fibers. Along the longitudinal direction, however, a continuous variation

of the shear within a bay is observed in all cases.

If the shears at the main spars determined from tests (fig. 20) are compared with those determined from the statically indeterminate computations, it is found that the test gives a somewhat larger concentration of the shear in the neighborhood of an applied force.

b) Transverse stress distribution.— The distribution of the transverse or circumferential stresses over the cylinder length and cylinder circumference is shown on figures 21 and 22. It was necessary to plot the ring stresses in the arching loading condition with unattached bulkheads e and f to a smaller scale since their maximum values were twenty times as great as the maximum values under the arching load with attached rings. In the polar coordinate representation, the compressive peripheral stresses are plotted outward in order that the radial loads produced by them in the stiffeners may be shown more clearly.

Under the bending loading condition, transverse stresses of importance occur only in bay V (between the reinforced bulkheads). The sign of the stresses does not change over the cylinder length. Under the arching loading condition, the transverse stresses become very small if the rings e and f are attached to the skin, and the stresses change sign several times over the cylinder length. If bulkheads e and f are unattached, the transverse stresses in bay V assume very large values, which are positive on the loading side (near ring f) and negative on the side of ring e. In the remaining bays the peripheral stresses remain insignificantly small.

The transverse stresses are obtained through the integration,

$$\sigma_y = \sigma_{y0} - \int_0^y \frac{\partial \tau}{\partial x} dy. \quad \text{The derivative } \frac{\partial \tau}{\partial x} \text{ on which the}$$

distribution of the magnitude of the peripheral stress essentially depends is obtained from equations (1) and (2). Differentiating equation (2) with respect to x, we obtain

$$\left(\frac{\partial \tau}{\partial x} \right)_b - \left(\frac{\partial \tau}{\partial x} \right)_a = - \frac{1}{s} \frac{d^2 P_x}{d x^2}$$

Differentiation of equation (1) for the sheet bays with respect to x gives

$$\frac{\partial^2 \tau}{\partial x \partial y} = - \frac{\partial^2 \sigma_x}{\partial x^2}$$

and by integrating over the periphery, there is obtained

$$\frac{\partial \tau}{\partial x} = \left(\frac{\partial \tau}{\partial x} \right)_0 - \int_0^y \frac{\partial^2 \sigma_x}{\partial x^2} dy$$

The derivatives $\frac{\partial \tau}{\partial x}$ therefore depend on the curvatures of the $\sigma_x(x)$ or $P_x(x)$ curves. The greatest transverse stresses in the cross sections will thus be expected to occur in those sections in which the $P_x(x)$ or $\sigma_x(x)$ curves are most sharply curved. If the bulkheads e and f are not attached to the skin the breaks (fig. 17) of the $P_x(x)$ curves at the bulkhead positions vanish and in their place, particularly between ring f and the center of bay V, there appear curve portions of very sharp curvature. This is the mathematical explanation for the high values of the transverse stresses. With unattached bulkheads no shears can be transferred locally. For this reason, the shear behind ring f in bay V (fig. 18) must sharply increase starting from zero. In the rear half of bay V, the shear decreases rapidly at first then more slowly. The internal equilibrium of the skin for such a stress distribution requires very high transverse stresses with change of sign in panel V.

c) The loading of the stiffener system.- The distribution of the longitudinal stresses along the cylinder is shown on figures 8 and 13 and that of the bulkhead stresses on figures 10 and 15. In the latter two figures are plotted the mean values of the stresses measured at the bulkheads and no effective supporting width of skin has been taken into account. The rings could be loaded tangentially through the transfer of the shear differences at rows of rivets between the bulkheads and skin, or radially through transferred peripheral forces of the peripheral

stresses. The flexurally very rigid "main spars" can have a loading as well as a supporting effect on the bulkheads.

If, in the bending case, the shell is cut along two lines symmetrical to the vertical center plane as shown on figure 11a, the cut section is acted upon not only by shear stresses but also by transverse stresses (indicated by thin lines). The bulkhead loading is therefore concentrated at the forward rings as is also shown by figure 10. A similar result is obtained in cutting along the vertical center plane, but in this case the couples in the two intersecting areas act in opposition to each other. Figure 23a shows the transverse loads on the main spar 12 due to the transverse stress components and their support against the rings. It follows that the stiff end ring contributes to this support.

In the case of the arching load with attached bulkheads (fig. 23b), the main spars are practically free from distributed loads, but they support the bulkhead *f*, which is highly loaded through tangential forces. They support themselves against the very weak bulkheads *a* to *d*, and this explains the strong bulging at the free end (fig. 12) as well as the high mean stresses in rings *a* to *c* (fig. 15). Tests have shown that the places where the main spars pass through the rings (figs. 1 and 12) are rather yielding in spite of bridging over connections.

In the case of the arching loading condition with rings unattached (fig. 23c), the main spars, on account of the high transverse stresses are acted upon by large transverse forces which change their signs over the length, the spars supporting themselves radially against the bulkhead rings on which there are no tangential forces. The bulging effect is essentially the same as with the attached bulkheads. If there is a stiff end ring the supporting forces of the spar concentrate themselves on this end ring and rings *a* to *d* are to a very large extent relieved of their load.

V. SUMMARY

In order to test the results and validity of the fundamental assumptions made in the computations by H. Ebner and H. Köller of the force distribution over cylindrical shells, stress measurements were made on a circular cylin-

drical shell loaded at four points. Two loading conditions were investigated, namely, a bending load and an "arching" load. From the measured longitudinal stresses the shears and the transverse stresses in the skin were obtained by integration of the fundamental equations of the two-dimensional stress field.

The measured stresses in the longitudinal stiffeners (stringers) are in satisfactory agreement with the computed values of Ebner and Köller for both loading conditions. The longitudinal stresses in the stiffeners between the "main spars" increase steadily, in the bending case, in the external fiber region from the loading end toward the fixed end. In the neighborhood of the neutral axis these stresses, after a rapid initial rise, attain a maximum and then decrease again to a value which corresponds to the linear stress distribution due to bending as a beam. In the arching type of loading condition, the stresses in the stiffeners between the main spars remain small.

The experimentally determined shears for the bending loading condition and arching loading condition with the two front bulkheads not attached to the skin were continuously distributed over the cylinder shell. In the arching loading condition with the two forward bulkheads riveted to the sheet, however, discontinuities arise in these bulkheads because the shears are transmitted to the bulkheads. In this case, comparison with the computed values gives a stronger concentration of the experimentally determined shears at the load application end. Within a bay the shears vary over the length. In the peripheral direction, however, they vary strongly under the bending load in the region of the extreme fibers. Near the neutral axis, however, they are practically constant along a strip. The same is true for the arching loading condition in all walls between the main spars.

The transverse stresses are small under the arching load if the first two bulkheads take up the shear differences as a result of their being riveted to the sheet. If the attachment to the skin is loosened, however, very high peripheral stresses are set up in the bay directly behind the force application (panel V) and these fluctuate greatly and change their signs within the bay. In the bending case, the peripheral stresses remain small.

The loading of the stiffener system depends essen-

tially on the flexural strength of the "main spars." In the arching type of loading with the two forward bulkheads riveted, the main spars transmit the force to the forward bulkhead in a radial direction. The support of the main spars on the flexurally weak bulkheads at the free end leads to a strong elliptical bulging of the latter. The same effect occurs as a result of the radial loading of the spars through the peripheral stress components if the forward bulkheads are not attached to the skin.

Riveting of the two forward bulkheads to the skin produces a somewhat more rapid rate of decrease of the forces in the main spars in the arching loading condition and the setting up of breaks in the curves of longitudinal force $P_x(x)$. The more rapid rate of decrease is to be explained by the fact that the skin contributes an effective supporting width when the bulkheads are under a bending load. The resistance of the shell against arching is not increased to any considerable extent by riveting since, with a stiff ring mounted at the end, the forces transferred from the main spars through the riveting are not changed by the riveting of the forward bulkheads. The end ring has the effect of strongly relieving the load from the bulkheads at the free end.

The buckling of the sheet had no effect in reducing the forces in the main spars within the range investigated (in bending, up to 2.5 times the buckling load and in arching, up to 1.8 times the buckling load).

The results of the tests suggest the necessity for an extension of the simple shear field by the addition of the transverse stresses and indicate that the bending strength of the stringers may be of considerable effect on the loading of the bulkheads.

The tests should be further extended to the case - more difficult to compute - where the cutaway of the shell lies only on one side and the shell at the side lying opposite is of framework construction.

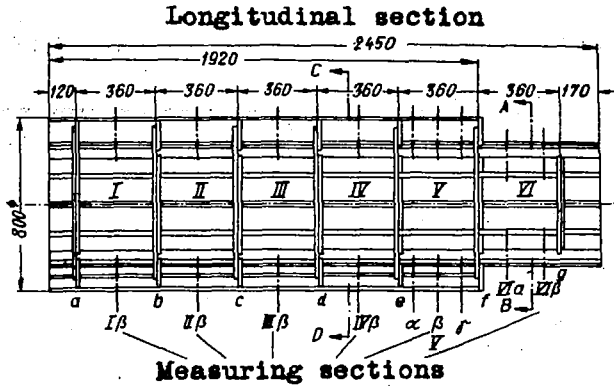
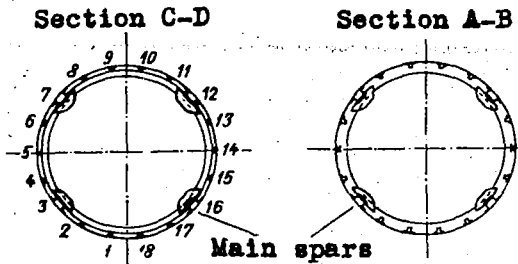
Translation by S. Reiss,
National Advisory Committee
for Aeronautics.

REFERENCES

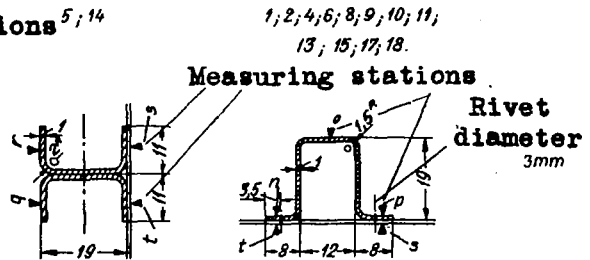
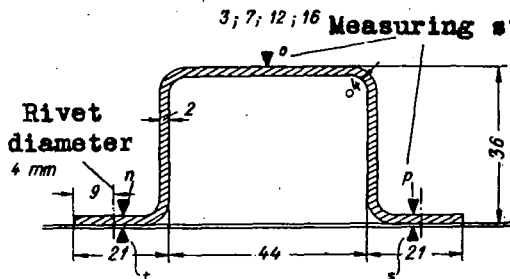
1. Ebner, H., and Köller, H.: Über die Einleitung von Langskraften in versteifte Zylinderschalen. Jahrbuch 1937 der deutschen Luftfahrtforschung. R. Oldenbourg 1937, München-Berlin.

Ebner, H., and Köller, H.: Calculation of the Load-Distribution in Stiffened Cylindrical Shells. T.M. No. 866, N.A.C.A., 1938.
2. Wagner, H., and Simon, H.: Über die Krafteinleitung in dünnwandige Zylinderschalen. Luftfahrtforschung, vol. 13, no. 9, 1936, pp. 293-308.
3. Ebner, H.: The Strength of Shell Bodies - Theory and Practice. T.M. No. 838, N.A.C.A., 1937.
4. Redshaw, C.: The Elastic Instability of a Thin Curved Panel Subjected to an Axial Thrust, Its Axial and Circumferential Edges Being Simply Supported. R. & M. No. 1565, British A.R.C., 1934.

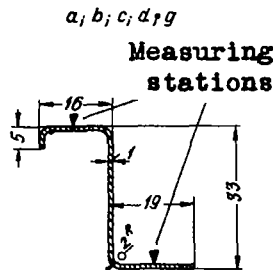
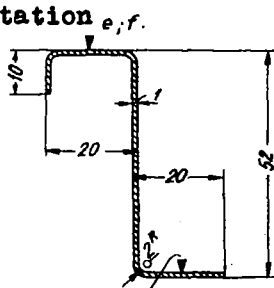
Sections through test cylinder.



Longitudinal stiffener sections



Bulkhead ring sections



Measuring station

Figure 1.- Test cylinder with stiffener sections.

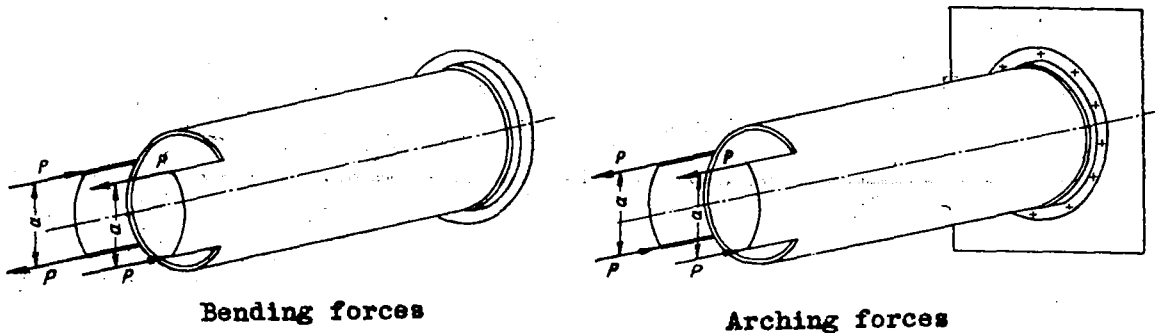


Figure 2.- Loading conditions.

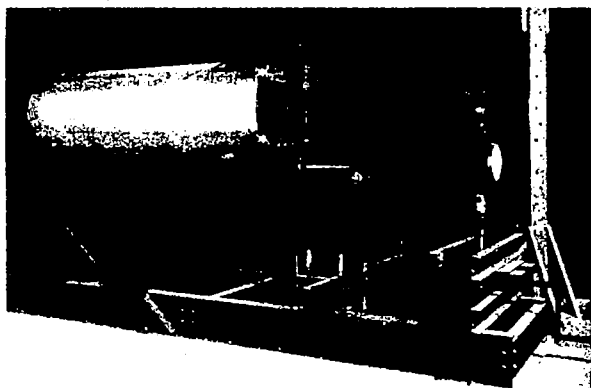


Figure 3.-Test set-up for bending loading condition

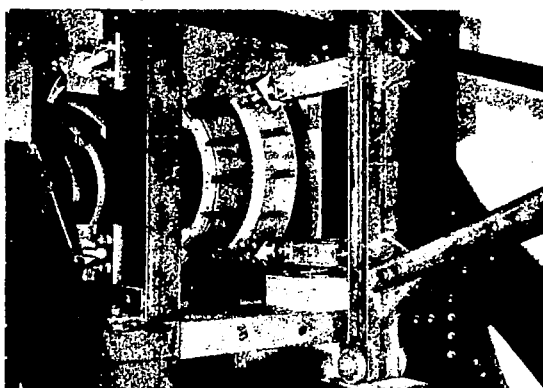


Figure 6.- Application of forces on test specimen under the arching loading condition.

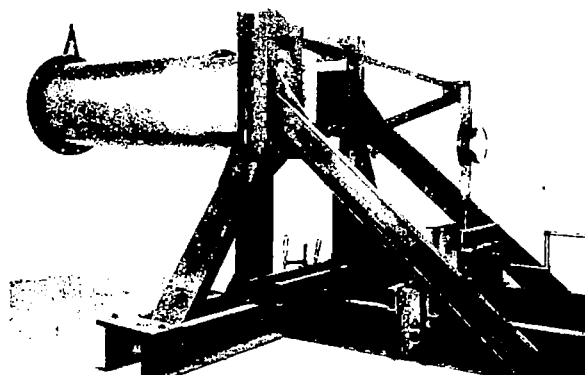


Figure 5.- Test set-up for arching loading condition.



Figure 12.- Bulging of the cylinder under an arching load.

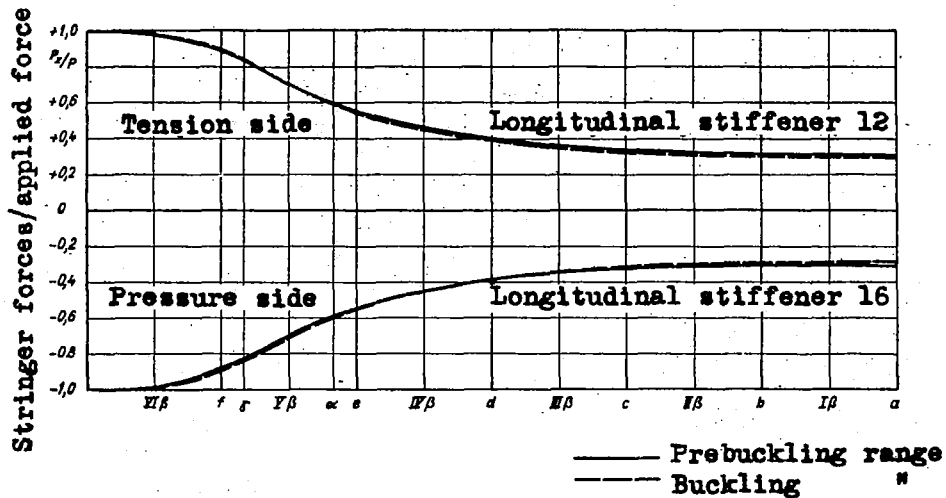


Figure 9.- Comparison of the main spar forces in the prebuckling and the buckling range for the bending loading condition.

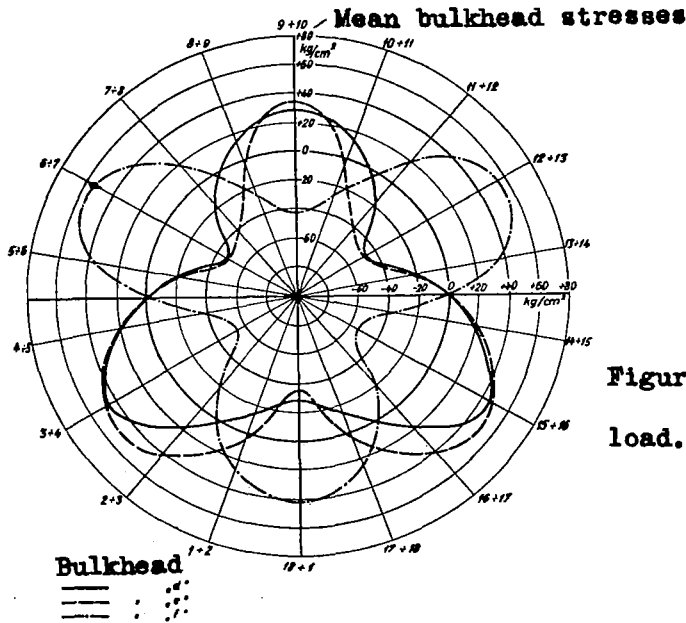


Figure 10.- Bulkhead stress under bending load.

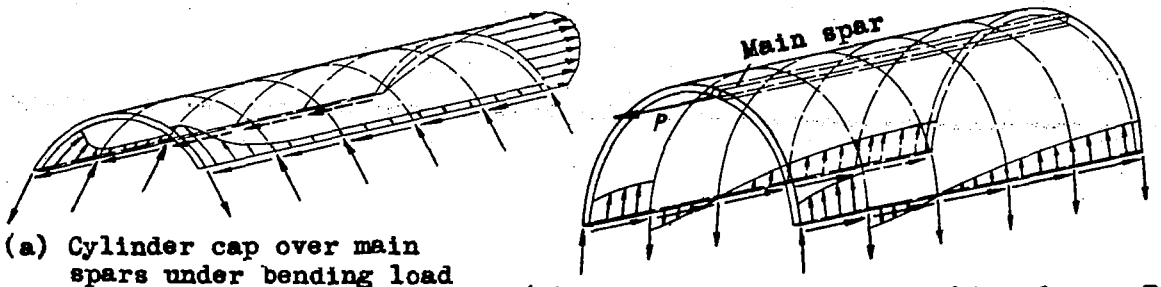


Figure 11.- Equilibrium of portions cut from the cylinder.

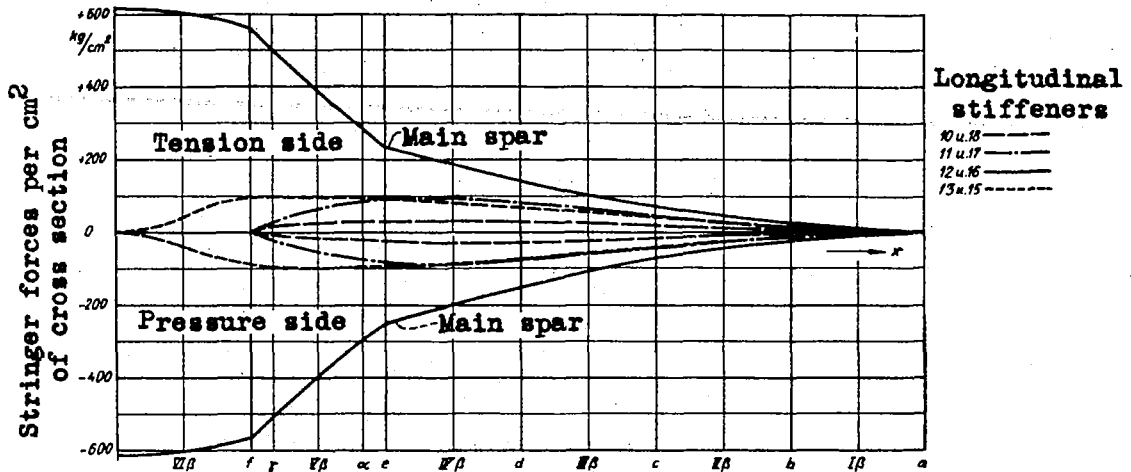


Figure 13.- Variation of stringer forces over the cylinder length under the arching loading condition.

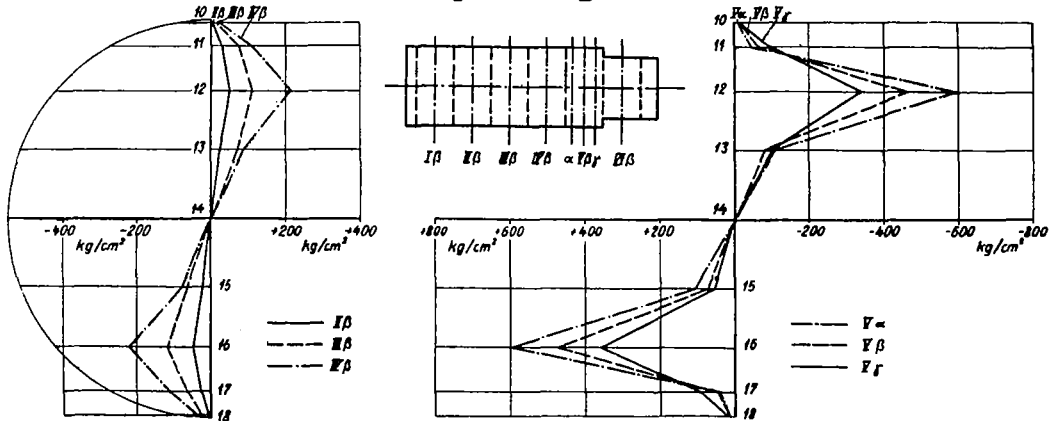


Figure 14.- Normal stress distribution over the cross section height under the arching loading condition.

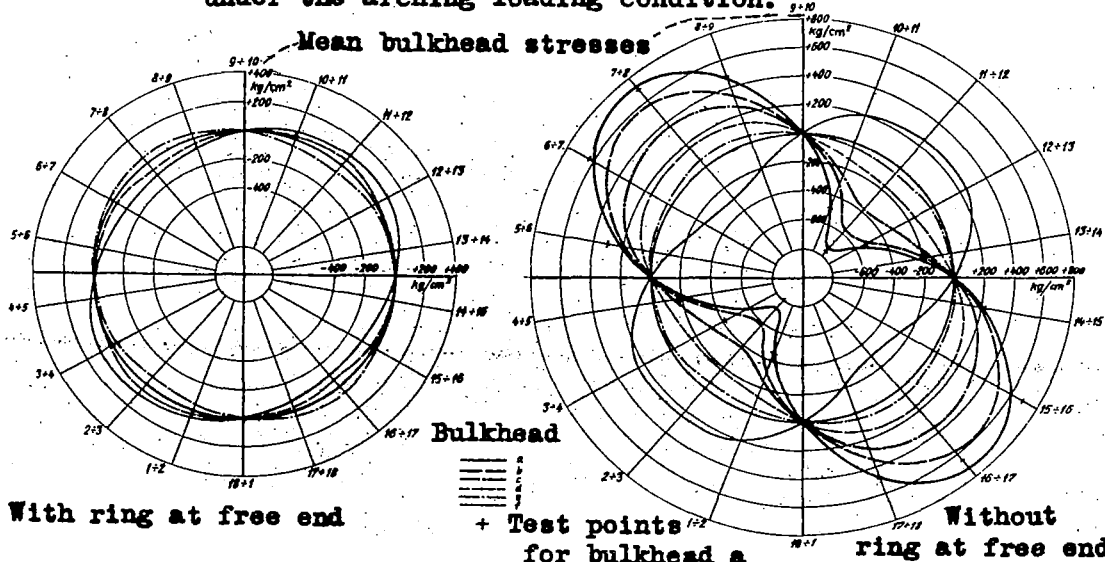


Figure 15.- Bulkhead ring stresses under the arching loading condition.

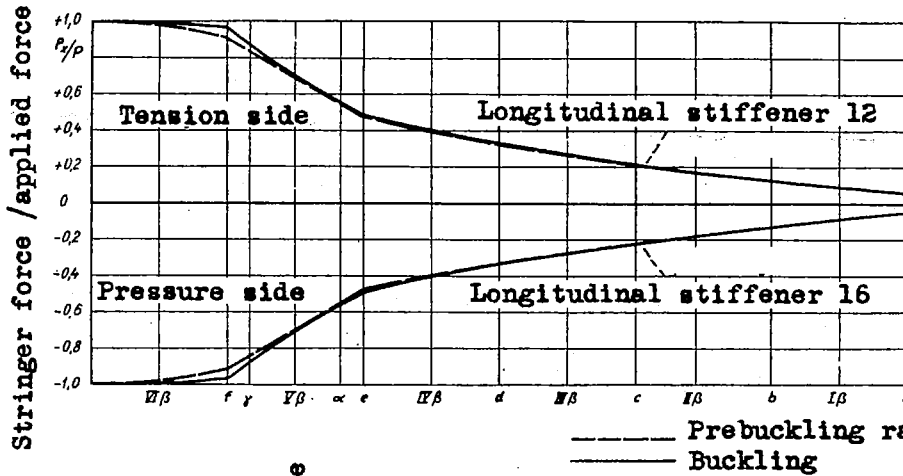


Figure 16.- Comparison of the main spar forces in the prebuckling and buckling range for the arching type of loading.

Figure 17.- Effect of a stiff end ring and of riveting of the bulkheads e and f on the force variation in the main spars.

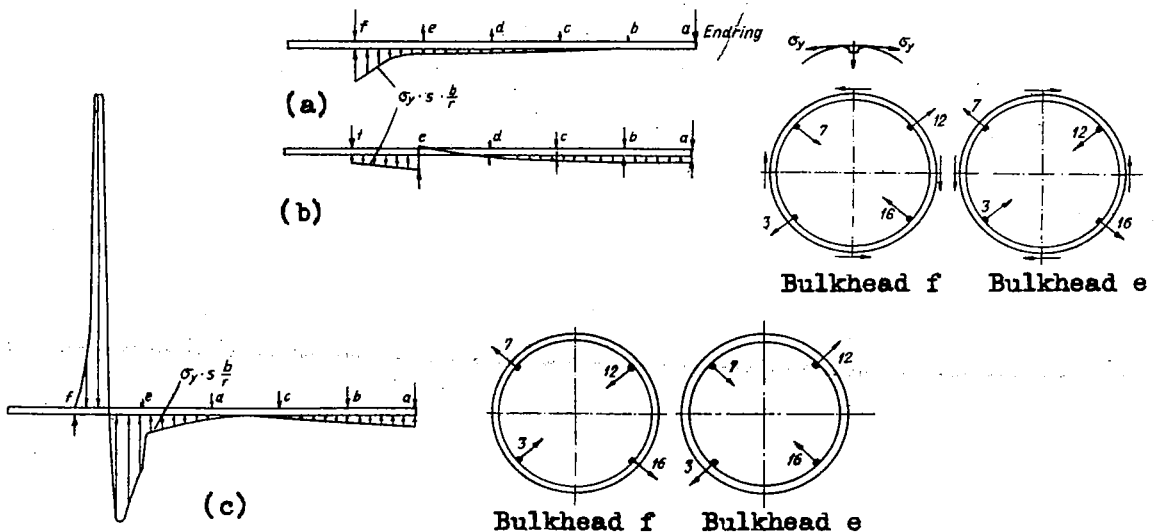
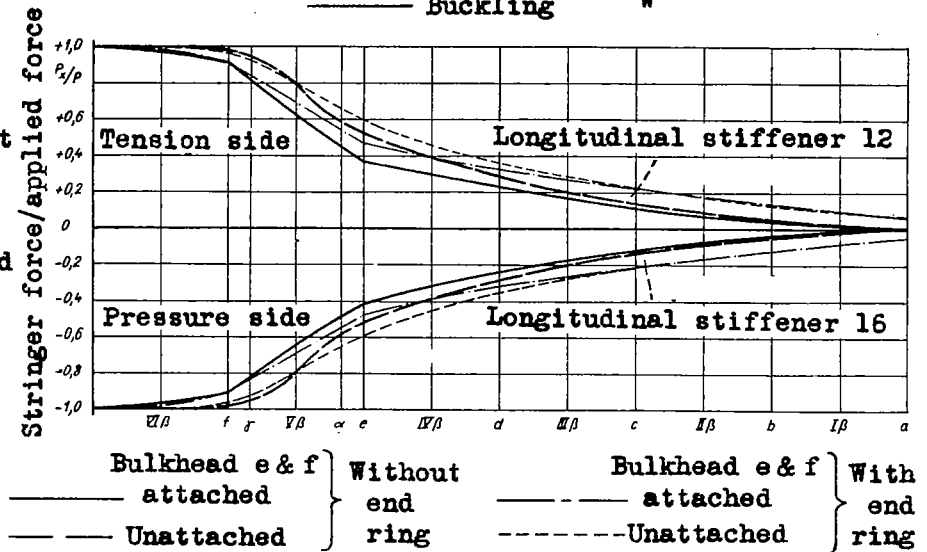
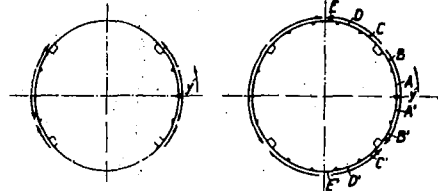
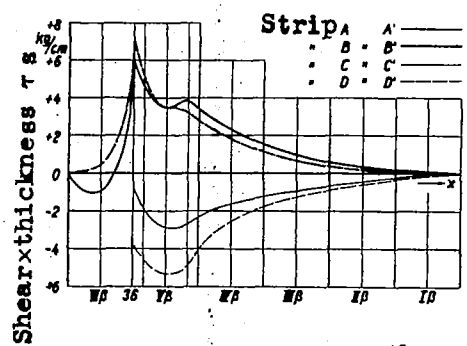
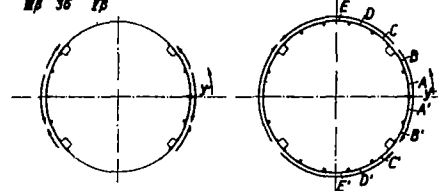
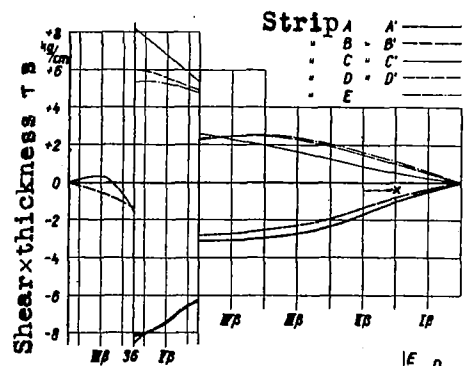


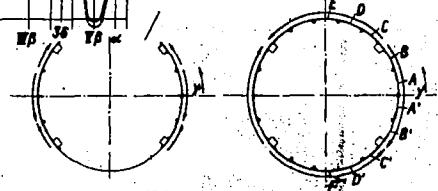
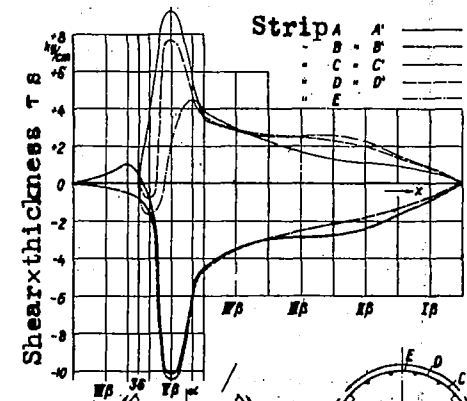
Figure 23.- Bending load of the main spars and bulkheads.



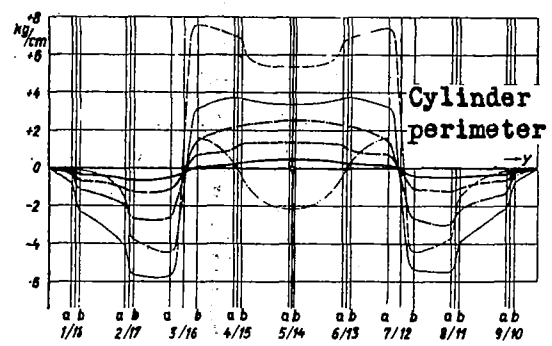
Section at VIβ Section at Vβ



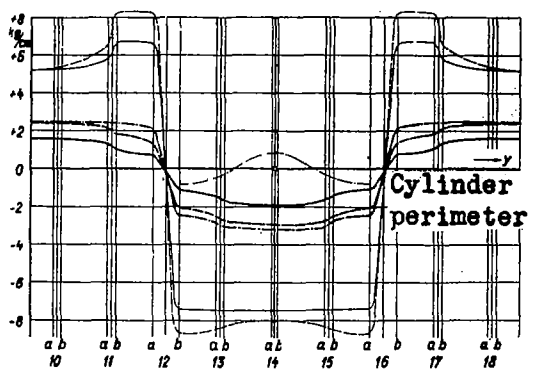
Section at VIβ Section at Vβ



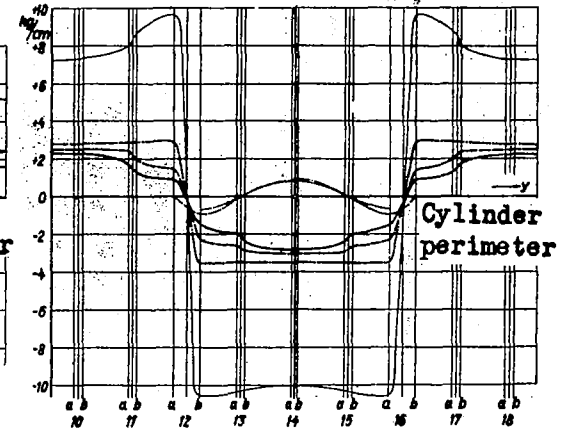
Section at VIβ Section at Vβ



Longitudinal stiffeners
Bending load



Longitudinal stiffeners.
Arching load with bulkheads
e and f riveted.



Longitudinal stiffeners.
Arching load with bulkheads
e and f unattached

Shear times

 thickness

 at sections

Figure 18.- Plot of the shear-times-thickness over the cylinder length and cylinder perimeter for P=1,000 kg

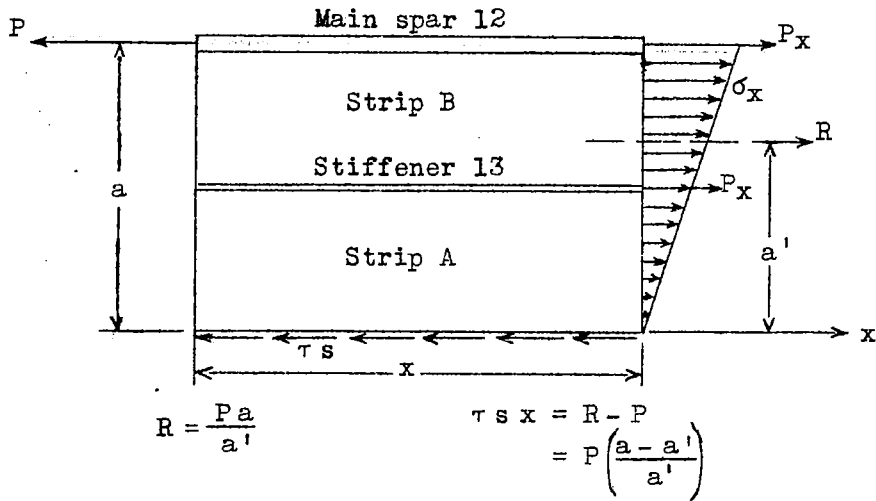


Figure 19.- Stress distribution in a wall at force application side.

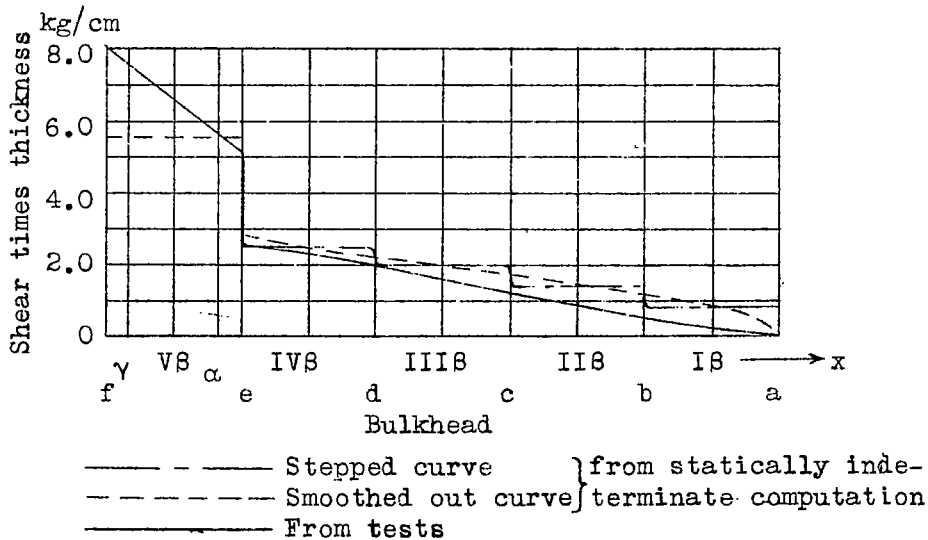


Figure 20.- Comparison of the shear times thickness at the main spars with the values obtained from the static computation.

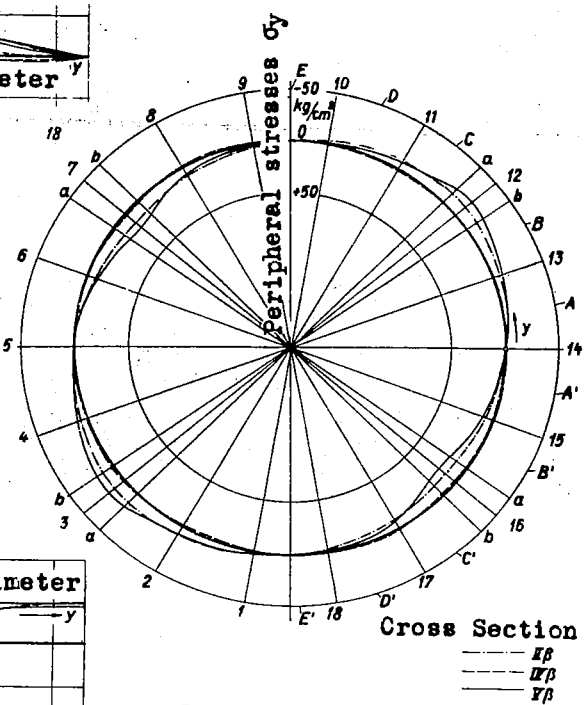
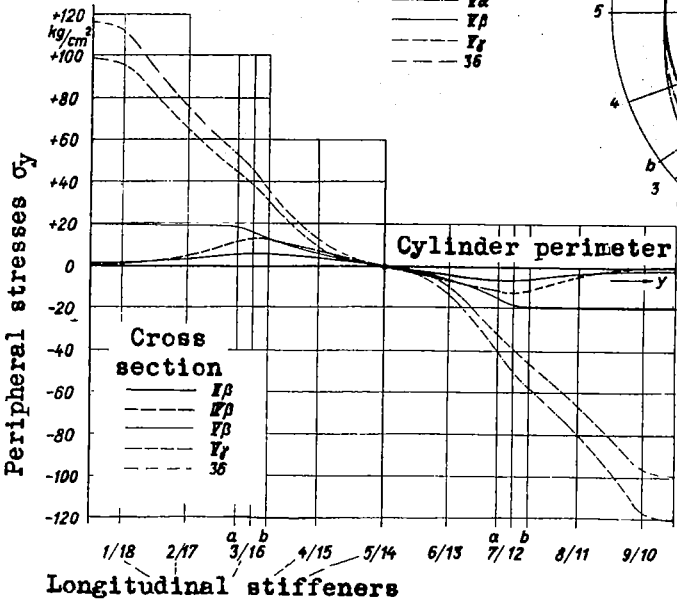
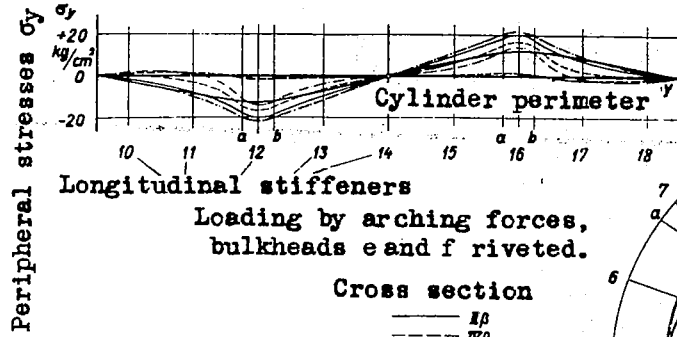
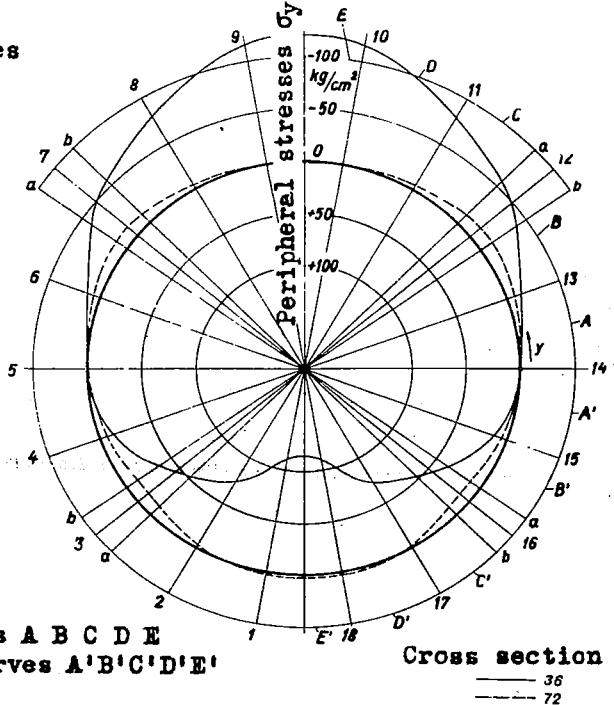
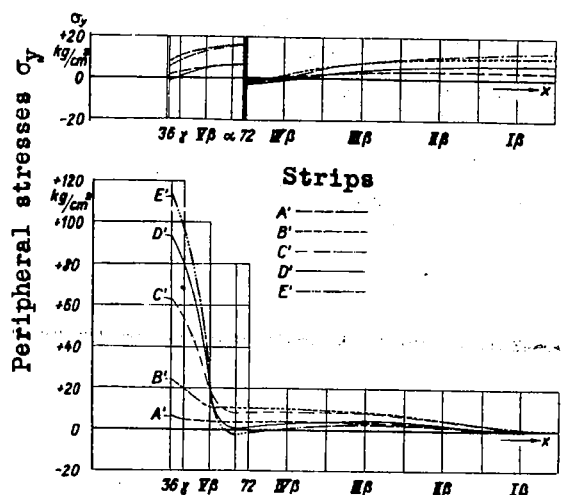
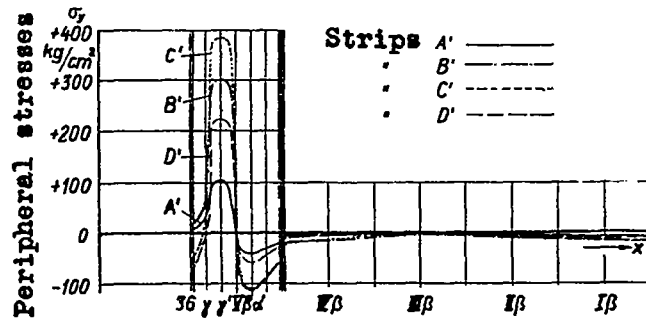


Figure 21.- Plot of the transverse stresses for $P=1,000\text{kg}$ (for the bending loading condition and for the arching loading condition with attached bulkheads)



The peripheral stresses in the strips A B C D E are obtained by reflection of the curves A'B'C'D'E' at x axis

Cross section
 — 36
 - - - 72



The peripheral stresses in the strips A B C D are obtained by reflection of the curves A'B'C'D'

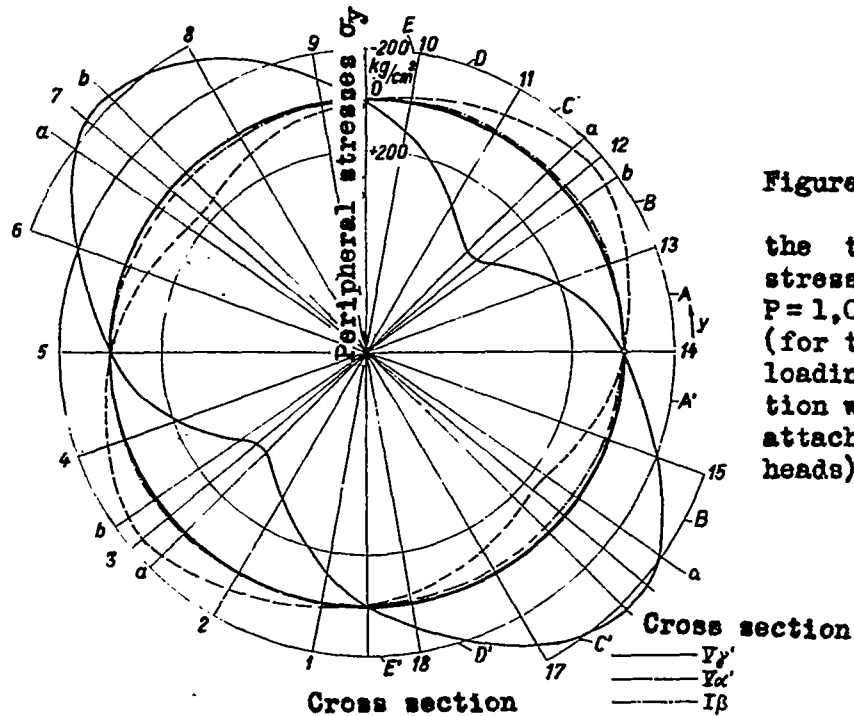
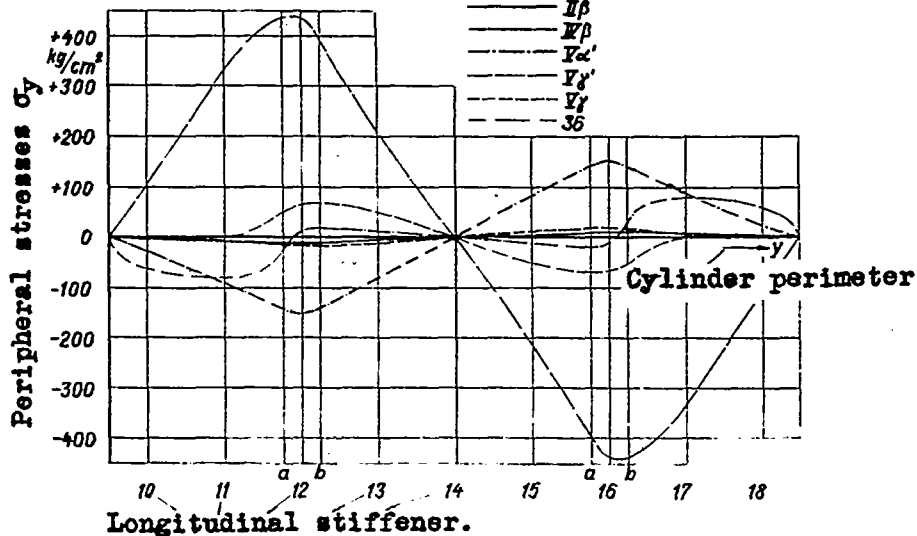


Figure 22.- Plot of the transverse stresses for $P=1,000$ kg (for the arching loading condition with unattached bulk-heads).



NASA Technical Library



3 1176 01440 3464